ARTICLES
https://doi.org/10.1038/s41564-020-0692-2
nature microbiology

Broad-spectrum anti-CRISPR proteins facilitate horizontal gene transfer

Caroline Mahendra[1], Kathleen A. Christie[2,3,4], Beatriz A. Osuna[1], Rafael Pinilla-Redondo[1,5,6], Benjamin P. Kleinstiver[2,3,4] and Joseph Bondy-Denomy[1,7,8] ✉

CRISPR–Cas adaptive immune systems protect bacteria and archaea against their invading genetic parasites, including bacteriophages/viruses and plasmids. In response to this immunity, many phages have anti-CRISPR (Acr) proteins that inhibit CRISPR–Cas targeting. To date, anti-CRISPR genes have primarily been discovered in phage or prophage genomes. Here, we uncovered *acr* loci on plasmids and other conjugative elements present in Firmicutes using the *Listeria acrIIA1* gene as a marker. The four identified genes, found in *Listeria, Enterococcus, Streptococcus* and *Staphylococcus* genomes, can inhibit type II-A SpyCas9 or SauCas9, and are thus named *acrIIA16–19*. In *Enterococcus faecalis*, conjugation of a Cas9-targeted plasmid was enhanced by anti-CRISPRs derived from *Enterococcus* conjugative elements, highlighting a role for Acrs in the dissemination of plasmids. Reciprocal co-immunoprecipitation showed that each Acr protein interacts with Cas9, and Cas9–Acr complexes were unable to cleave DNA. Northern blotting suggests that these anti-CRISPRs manipulate single guide RNA length, loading or stability. Mirroring their activity in bacteria, AcrIIA16 and AcrIIA17 provide robust and highly potent broad-spectrum inhibition of distinct Cas9 proteins in human cells (for example, SpyCas9, SauCas9, SthCas9, NmeCas9 and CjeCas9). This work presents a focused analysis of non-phage Acr proteins, demonstrating a role in horizontal gene transfer bolstered by broad-spectrum CRISPR–Cas9 inhibition.

Bacteria are constantly exposed to invasive mobile genetic elements (MGEs) that can either benefit or harm the host. Many MGEs encode antibiotic resistance pathogenicity factors that can enhance microbe virulence[1,2]; however, most are regarded as parasitic entities[3]. To combat MGE invasions, bacteria possess defence mechanisms, including restriction modification and CRISPR–Cas adaptive immunity[4], which can limit the exchange of destructive genetic material[5–7]. CRISPR–Cas systems are widespread, found in roughly half of bacteria and over 80% of archaea[8], and can protect host genomes against phage infection and plasmid conjugation[9]. Yet, occurrence of horizontal gene transfer (HGT) persists across species, which is evident by DNA sequence estimates suggesting that, on average, 5–6% of genes in bacterial genomes are derived from HGT[10], with numbers as high as 10–20% for some microbes[11].

Bacteriophages have responded to CRISPR–Cas with anti-CRISPR (Acr) proteins[12], which can inhibit CRISPR–Cas complex formation/stability[13,14] or target DNA binding or cleavage[15–18]. To date, 46 distinct Acr protein families inhibiting various CRISPR–Cas subtypes have been discovered, in which type II-A Cas9 inhibitors alone constitute 11 (refs. [19–23]). Numerous strategies have been employed for Acr discovery, including bioinformatic[19,24], experimental[12,20] and metagenomic screening[22,23]. Many of these approaches have discovered Acrs on phages and prophages; however, it is not clear how other MGEs avoid CRISPR targeting.

Here, we utilize the widespread phage and plasmid-encoded *acrIIA1*, previously identified in *Listeria* prophages, as a marker gene to discover four distinct inhibitors of the type II-A CRISPR–Cas system, named *acrIIA16–19*. These proteins are predominantly encoded by non-phage elements, including plasmids and integrative and conjugative elements. We demonstrate that AcrIIA16–19 inactivate Cas9-mediated cleavage of foreign DNA in vivo during phage infection and plasmid conjugation, in vitro and in human cells. In vitro analyses suggest that these inhibitors interact with SpyCas9 through mechanisms distinct from the DNA mimics AcrIIA2 (refs. [25,26]) and AcrIIA4 (refs. [27,28]) and may modulate single guide RNA (sgRNA) expression, stability or loading. Interestingly, AcrIIA16 displays broad-spectrum inhibition of SpyCas9 and SauCas9, similar in potency to previously identified AcrIIA5 (refs. [21,29]), while AcrIIA17 potently inhibits type II-C NmeCas9. Together they provide useful off switches for multiple phylogenetically distinct Cas9s.

Results

Type II-A anti-CRISPRs (AcrIIA16–19) inhibit SpyCas9 upstream of DNA binding. To better understand how MGEs interact with CRISPR–Cas immunity, we sought to identify undiscovered *acr* genes. We utilized the widespread *acrIIA1* gene as an anchor in bioinformatic searches across genomes on NCBI (Fig. 1a). An AcrIIA1 homologue (41% amino acid sequence identity) was previously identified within a *Listeria monocytogenes* plasmid, along with an AcrIIA2 homologue that was recently characterized (AcrIIA2b.3, Jiang et al.[25]). Genomic neighbours in this locus were tested against the type II-A Cas9 system using an established SpyCas9 phage-targeting screening system in *Pseudomonas aeruginosa*[25,30] (Fig. 1b). Gene *AWI79_RS12835* (now *acrIIA16*) inhibited SpyCas9 in this assay. Using *acrIIA16* as the anchor gene, testing of its neighbours revealed three more distinct anti-CRISPR genes (*acrIIA17–19*) identified in *Enterococcus*, *Streptococcus* and *Staphylococcus* (Fig. 1a). To quantify the strength of SpyCas9 inhibition, Cas9 and the sgRNA

[1]Department of Microbiology and Immunology, University of California, San Francisco, San Francisco, CA, USA. [2]Center for Genomic Medicine, Massachusetts General Hospital, Boston, MA, USA. [3]Department of Pathology, Massachusetts General Hospital, Boston, MA, USA. [4]Department of Pathology, Harvard Medical School, Boston, MA, USA. [5]Section of Microbiology, University of Copenhagen, Universitetsparken 15, Copenhagen, Denmark. [6]Department of Technological Educations, University College Copenhagen, Sigurdsgade 26, Copenhagen, Denmark. [7]Quantitative Biosciences Institute, University of California, San Francisco, San Francisco, CA, USA. [8]Innovative Genomics Institute, Berkeley, CA, USA. ✉e-mail: joseph.bondy-denomy@ucsf.edu

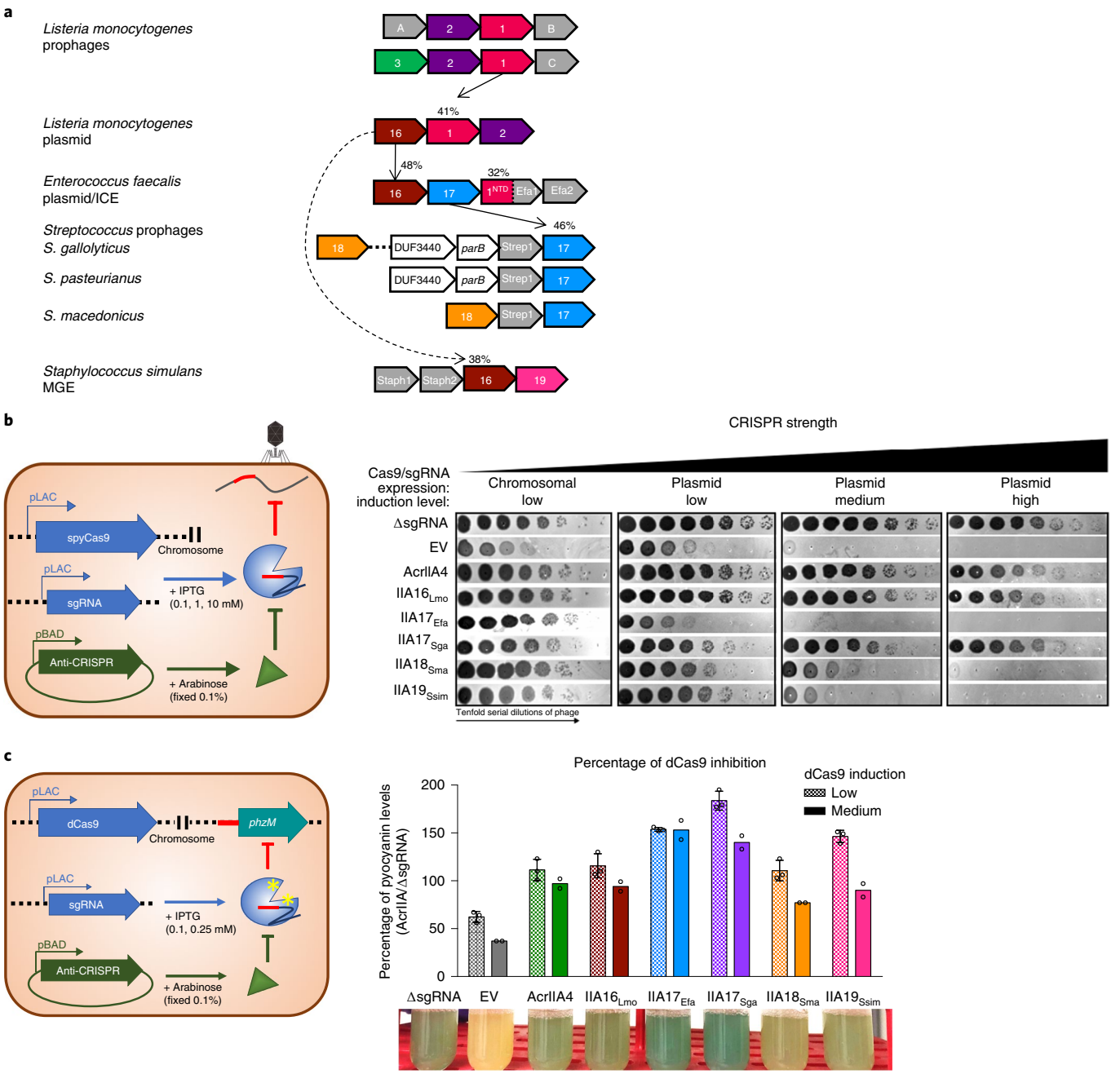

Fig. 1 | Identification of four type II-A Cas9 inhibitors, AcrIIA16–19. a, Schematic representation of type II-A *acr* genes, with vertical arrows indicating relationships between *acr* loci and percent protein sequence identity. Numbers in genes correspond to AcrIIA number. Grey genes are proteins of unknown function that tested negative for AcrIIA activity. ICE, integrative and conjugative elements. **b**, Schematic of phage plaque assays to assess CRISPR–SpyCas9 inhibition. Tenfold serial dilutions of targeted phage (black circles) are spotted on a lawn of *P. aeruginosa* (grey background) expressing the type II-A CRISPR–Cas system and indicated *acr* genes. CRISPR strength is determined by expression of sgRNA from the chromosome (low), or from a multicopy plasmid at increasing induction levels (0.1, 1 and 10 mM IPTG). ΔsgRNA lacks a phage-targeting sgRNA. EV, empty vector. Representative picture of at least three biological replicates for each are shown. **c**, Schematic of experiment to assess CRISPRi inhibition. Chromosomally integrated dCas9 (yellow asterisks) in *P. aeruginosa* programmed to bind the *phzM* gene promoter with sgRNA expressed from a multicopy plasmid at low or medium IPTG induction levels, in the presence of indicated AcrIIA proteins. CRISPRi inhibition was assessed by quantification of pyocyanin levels in response to *phzM* gene repression, relative to ΔsgRNA. Percentage pyocyanin levels at low and medium CRISPR strength are represented as the mean of three ± s.d. and two biological replicates, respectively, and a representative picture at medium CRISPR strength is shown (bottom).

were titrated via isopropyl-*b*-D-thiogalactoside (IPTG) induction. At the lowest CRISPR–Cas expression level, all identified *acrIIA* genes inhibited SpyCas9, restoring phage replication to nearly the same levels as in the strain lacking CRISPR immunity (ΔsgRNA indicates absence of sgRNA, Fig. 1b). However, at higher CRISPR–Cas expression levels, only AcrIIA16$_{Lmo}$ (where subscripted Lmo indicates the strain *Listeria monocytogenes*), AcrIIA17$_{Sga}$ (where subscripted Sga indicates the strain *Streptococcus gallolyticus*) and

control AcrIIA4 maintained inhibition against SpyCas9 (Fig. 1b). In agreement with this result, the AcrIIA proteins also protect against self-genome cleavage assay with a similar strength (Extended Data Fig. 1b).

To inspect the mechanism of these AcrIIA proteins in vivo, we established a CRISPRi assay, where catalytically dead SpyCas9 (dCas9) is programmed to bind the promoter of the *phzM* gene. Repression of *phzM* halts the production of a green pigment called pyocyanin, generating a yellow culture[15]. In the presence of AcrIIA4, DNA binding by dCas9 is inhibited, generating a green culture. AcrIIA16–19 all presented a similar phenotype to AcrIIA4, at two dCas9 induction levels, suggesting that these AcrIIAs inhibit SpyCas9 at the step of target DNA binding or at an upstream stage (Fig. 1c).

***acrIIA* genes inhibit Cas9 during conjugation.** To determine the distribution of the identified acr loci, adjacent genes were examined for the presence of signature genes that denote the locus to be phage, plasmid, MGE-like or chromosome (see Methods for details). A comprehensive list of Acr orthologues is listed in Supplementary Table 2. Analysis of AcrIIA16–18 distribution revealed that most orthologues are present in conjugative MGEs, with some found in phages, bacterial chromosomes or other mobile elements including transposons or integrons (Fig. 2a). AcrIIA16 is widespread in plasmids or integrative and conjugative elements of various Firmicutes. AcrIIA17 is equally distributed in plasmids and prophages, predominantly found in *Streptococcus* and *Lactococcus* species. Full-length AcrIIA18 is commonly found on *Streptococcus* and *Staphylococcus* prophages, while it's C-terminal domain is not only found on a *Streptococcus* phage, but also on plasmids and core genomes of other Firmicutes (for example, *Clostridium* sp. and *Paeniclostridium* sp.) and *Azospirillium* sp. (*Proteobacteria*). AcrIIA19$_{Ssim}$ was initially identified on a plasmid, but its homologues are commonly found in *Staphylococcus* prophages. Moreover, it possesses a helix-turn-helix domain, reminiscent of AcrIIA1, suggesting a dual regulatory and anti-CRISPR function[31]. Altogether, these Acr proteins are encoded by a variety of microbes and mobile elements, including phages, plasmids and conjugative elements.

Given the prevalence of many of these genes on plasmids, we chose to investigate the plasmid-encoded *acrIIA16*, *17* and *19* orthologues against CRISPR targeting during plasmid conjugation. We tested the ability of Cas9 to target a plasmid when an AcrIIA protein is expressed either in the recipient or by the conjugating element. Previously reported *Enterococcus faecalis* strains[32] were engineered to express *acrIIA* genes individually from an *E. faecalis* promoter native to the *acr* locus. *E. faecalis* encodes two distinct endogenous type II-A CRISPR–Cas variants—CRISPR1, which is 52% identical to SpyCas9, and CRISPR3, which is 32% identical to SauCas9 (Fig. 2b). Two different conjugating plasmids were used, each engineered to contain a protospacer matching a natural spacer found in recipient cells OG1RF (CRISPR1) or T11RF (CRISPR3). Conjugation efficiency was reduced by 100–500-fold due to Cas9 targeting (Fig. 2c). When *acrIIA16*, *17* or *19* were pre-expressed in recipient cells, all inhibited CRISPR1 robustly, and CRISPR3 to a lesser degree (Fig. 2c and Extended Data Fig. 3a). *acrIIA4* only inhibited CRISPR1 activity, which encodes a Cas9 that has a similar protospacer adjacent motif (PAM)-interacting domain to SpyCas9 (Fig. 2c).

To determine whether AcrIIA proteins could function when the conjugating CRISPR-targeted plasmid carries the *acrIIA* gene, the targeted plasmids were engineered to express *acrIIA16–17* or *acrIIA19* from a native *Enterococcus acr* promoter. These *acr* genes were indeed protective against plasmid targeting by CRISPR1 when produced during conjugation, with *acrIIA17* providing modest protection against CRISPR3 (Fig. 2d and Extended Data Fig. 3b). Oddly, plasmids expressing certain *acr* genes did not produce detectable transconjugants (for example, *acrIIA17*$_{Efa}$ (where subscripted *Efa* indicates the strain *Enterococcus faecalis*) when challenged with CRISPR1, and *acrIIA4*/*acrIIA19*$_{Ssim}$ (where subscripted *Ssim* indicates the strain *Staphylococcus simulans*) against CRISPR3), but this was independent of CRISPR targeting (Extended Data Fig. 3c) for a reason that is unknown. We conclude that *acrIIA* genes are able to inhibit both CRISPR–Cas9 systems during plasmid conjugation in *E. faecalis* and can enhance HGT by >1 order of magnitude when pre-expressed in recipient cells.

AcrIIA16–19 proteins interact with SpyCas9. To further investigate the mechanism of Cas9 inhibition by the AcrIIA proteins, we purified one homologue of AcrIIA16–19 to directly test their effect on SpyCas9 activity. Surprisingly, in vitro cleavage experiments using the purified AcrIIA16–19 proteins and guide-loaded SpyCas9 did not directly inhibit DNA binding or cleavage under these conditions, while the positive control AcrIIA4 did (Fig. 3a). Due to the CRISPRi results above, suggesting that a step upstream of DNA binding could be inhibited, we next considered guide RNA stability or loading. Total RNA was harvested from the *P. aeruginosa* strains co-expressing SpyCas9, sgRNA and Acr proteins, followed by probing for sgRNA with a Northern blot (Fig. 3b, two independent biological replicates are shown). Interestingly, sgRNA in cells expressing AcrIIA16 are visible as two distinct bands—full length and a shorter version relative to its wild-type length. The presence of AcrIIA17 and AcrIIA19 leads to undetectable sgRNA in the cell, while presence of AcrIIA18 induces a slightly truncated sgRNA. These results suggest inhibition mechanisms for AcrIIA16–19 that may involve manipulation of sgRNA levels or loading. To test whether any of the Acr proteins can directly interfere with sgRNA loading, the in vitro cleavage experiment was repeated, but with AcrIIA proteins first incubated with sgRNA before complexing with ApoSpyCas9. Remarkably, this change enabled inhibition by AcrIIA16, blocking SpyCas9-mediated DNA cleavage (Fig. 3c). AcrIIA17–19 activity was unaffected by this change in protocol. This suggests that AcrIIA16 acts on the sgRNA, ApoCas9 or both to prevent activity.

Fig. 2 | Prevalence of *acrIIA* genes in integrative MGEs and their effect on CRISPR targeting during conjugation. a, Left: host distribution of *acrIIA16–19* based on phylogenetic analysis, see Extended Data Fig. 2. CFB, *Cytophaga*, *Fusobacterium* and *Bacteriodes*. Right: MGE distribution of *acrIIA16–19* based on genomic neighbours characteristic of phage, plasmid, chromosomal or mobile genes including transposons and integrons. 'Unclear' denotes genomic regions that could not be identified as known elements. For every genomic region, at least one signature gene is identified to characterize the MGE type, see Methods and Supplementary Table 2 for details. **b**, Schematic of the native CRISPR–Cas system in *E. faecalis* strains OG1RF for CRISPR1 and T11RF for CRISPR3 utilized for all conjugation experiments. Black diamonds denote spacers in the CRISPR array and the red diamonds indicate the spacers that match the engineered protospacers in the targeted plasmids. **c**, Schematic of conjugation in *E. faecalis* encoding a type II-A CRISPR system that targets the protospacer-bearing plasmid in the presence of indicated *acrIIA* genes episomally expressed in recipient cells. Conjugation frequency is quantified as transconjugants per donor relative to a non-targeted plasmid, and represented as the mean of three biological replicates ± s.d. **d**, Schematic of plasmid conjugation in *E. faecalis* from a donor to recipient. The conjugating plasmid carries the indicated *acrIIA* gene and is targeted by the host's type II-A CRISPR–Cas system. Conjugation frequency is quantified as transconjugants per donor relative to a non-targeted plasmid, and represented as the mean of three biological replicates ± s.d. ND, no colonies detected.

To determine whether AcrIIA16–19 interact with Cas9, myc-tagged SpyCas9 was immunoprecipitated from the *P. aeruginosa* strains introduced above. This experiment revealed that all four AcrIIA proteins copurify with SpyCas9 (Fig. 4a). Interestingly, SpyCas9 purified from cells co-expressing AcrIIA17–19 did not perform DNA cleavage. The absence of any obvious stoichiometric,

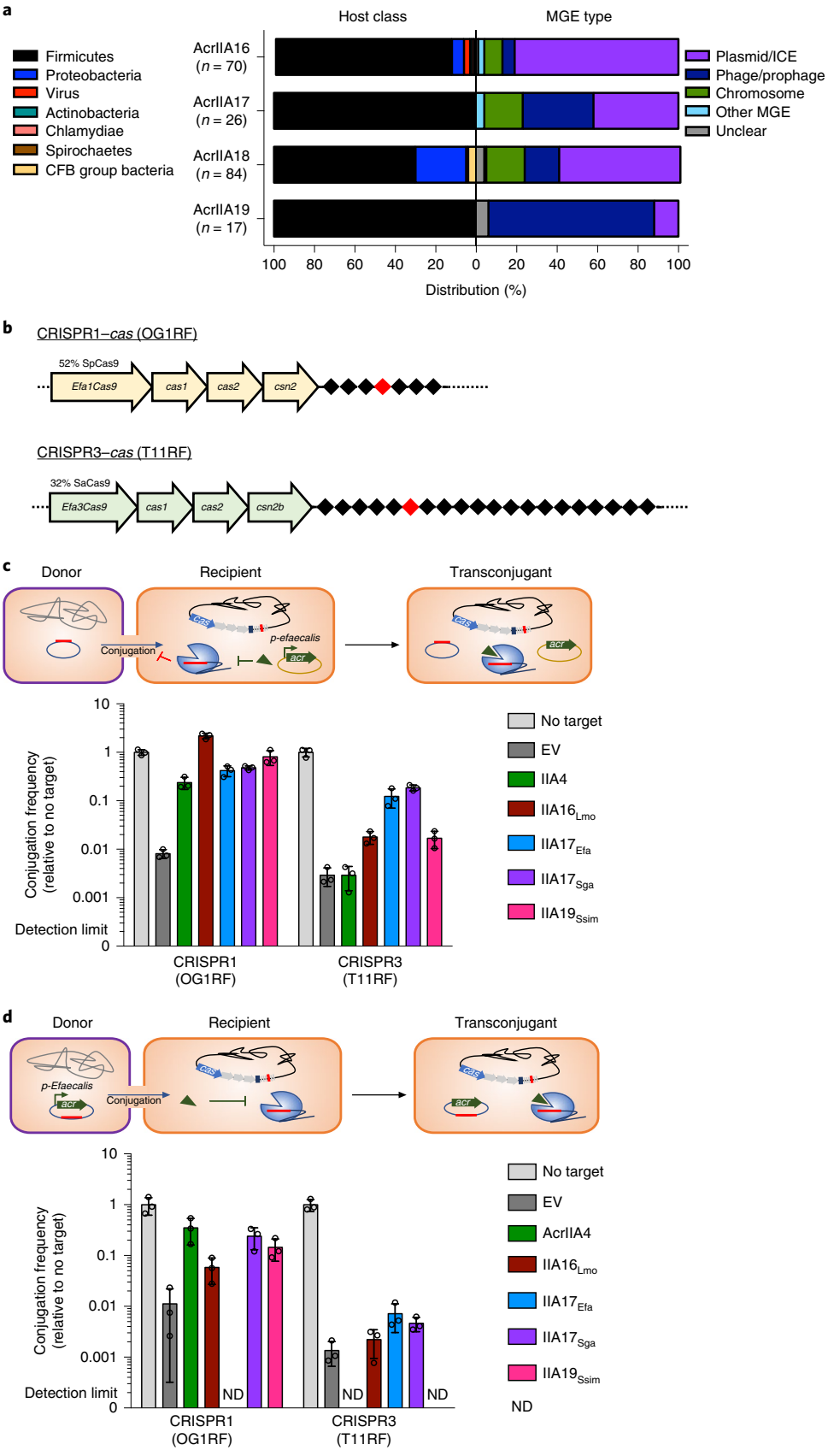

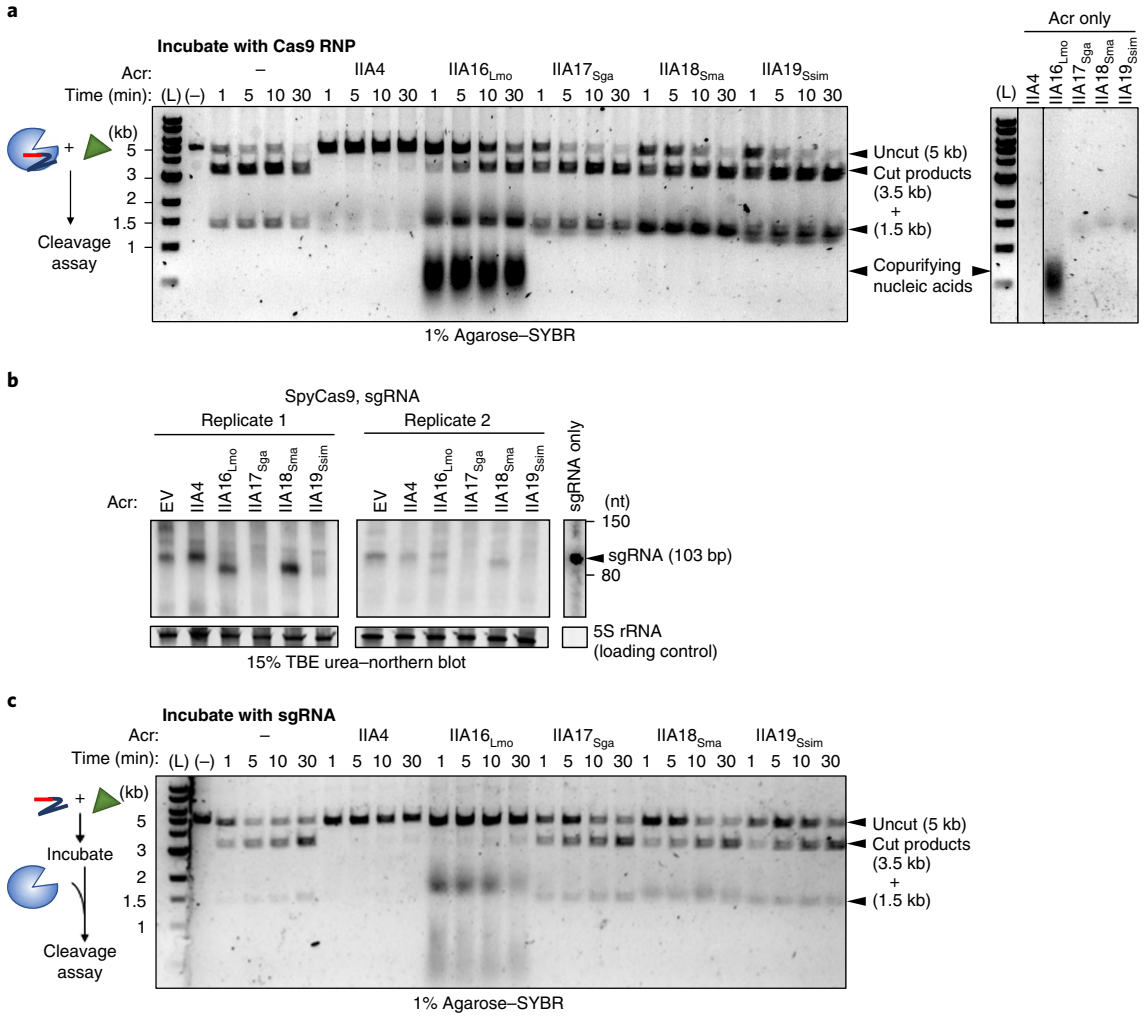

Fig. 3 | In vitro binding and inhibition activities of AcrIIA16–19 against SpyCas9. a, Left: time courses of prebound SpyCas9-sgRNA cleavage reactions targeting a double-stranded linear DNA template in the presence of purified Acr proteins. Right: purified Acr proteins loaded on agarose gel to visualize the presence of copurifying nucleic acids. Data shown are representative of two replicates. **b**, Northern blot analysis of sgRNA in *P. aeruginosa* expressing SpyCas9-sgRNA and indicated Acrs. For all blots, 5S ribosomal RNA served as loading control. Data are shown for two independent experiments. **c**, Time courses of target DNA cleavage reactions using sgRNA preincubated with Acr proteins followed by ApoSpyCas9 to form RNP. Representative timepoints are shown at the top of each lane. Data shown are representative of two replicates. (L), 1-kilobase (kb) double-stranded DNA ladder; (–), DNA template alone.

copurifying proteins suggests a direct interaction between Cas9 and the Acr proteins (Extended Data Fig. 4b). SpyCas9 copurified with low amounts of AcrIIA16$_{Lmo}$; however, it was not inhibited (Fig. 4b). The failure of AcrIIA16$_{Lmo}$ to inhibit immunoprecipitated SpyCas9 in vitro may be due to its low expression level, as visualized in the western blot input (Fig. 4a) and/or the fact that it inhibits when exposed to the sgRNA first. Northern blot also suggested that traces of wild-type-length sgRNA are still present in cells expressing AcrIIA16$_{Lmo}$ (Fig. 3b), which could form active RNP.

We next conducted the reciprocal co-immunoprecipitation experiment, confirming that SpyCas9 co-purifies with each tagged Acr (Fig. 4c). Moreover, we observed that SpyCas9 expressed in *P. aeruginosa* exhibits a series of degradation products when blotted for the C-terminal Myc tag. The enriched SpyCas9 fragments co-immunoprecipitated with AcrIIA16–19 appeared to be different from those of AcrIIA4, suggesting distinct binding sites (Fig. 4c). This experiment, coupled with observations of sgRNA degradation led us to test whether these Acr proteins bind ApoSpyCas9, which is a complex previously reported to be only a weak AcrIIA4 binding partner[28] and strong in vitro interaction partner for AcrIIA1 (ref. [31]). AcrIIA16–17 and AcrIIA19 copurified with ApoSpyCas9 similar to expected levels of AcrIIA1. AcrIIA4 showed weak binding (comparing the relative amount of AcrIIA4 to Cas9) and AcrIIA18 showed no interaction with ApoSpyCas9 (Fig. 4c and Extended Data Fig. 4d). These results suggest that AcrIIA16, 17 and 19 have distinct SpyCas9 interacting mechanisms compared to AcrIIA4 and AcrIIA18, and may modulate sgRNA stability or loading via an interaction with ApoCas9.

AcrIIA16$_{Efa}$ and AcrIIA17$_{Efa}$ potently inhibit Cas9 orthologues in human cells. Given the increasing use of various Cas9 orthologues for gene editing applications, we examined the ability of our AcrIIA proteins to prevent SpyCas9 activity in human cells. HEK293T cells were cotransfected with plasmids expressing Cas9, sgRNAs programmed to target sites located in endogenous genes and 13 different *acrIIA* genes—two homologues each for AcrIIA16–19 along with five previously validated control *acr* genes. By using targeted deep sequencing to evaluate editing activity, we observed near-complete inhibition of SpyCas9 by the two AcrIIA16 orthologues at levels comparable with the well-validated AcrIIA4 (refs. [27,28]) and the

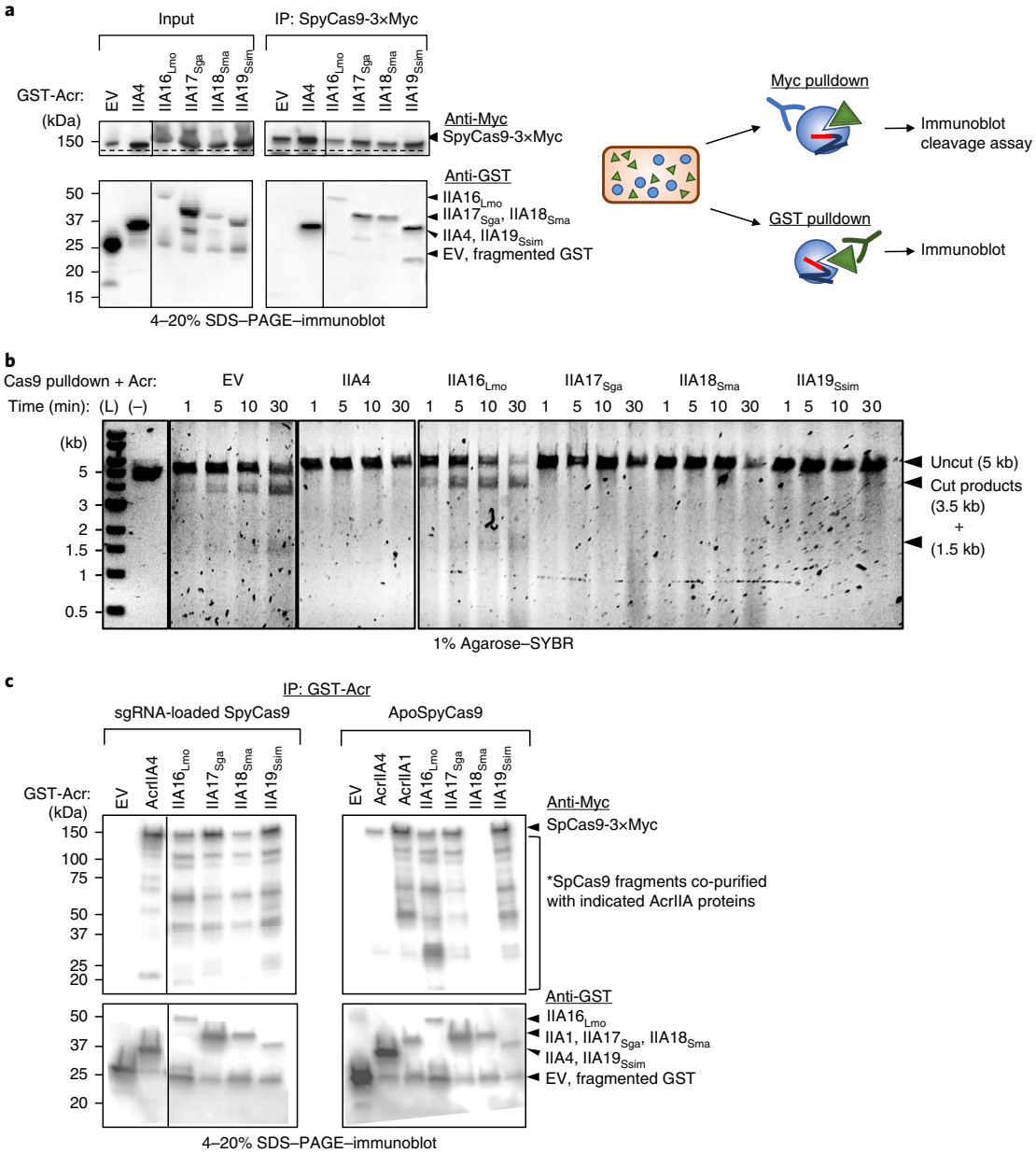

Fig. 4 | In vivo co-immunoprecipitation of AcrIIA16–19 and SpyCas9. a, Immunoprecipitation (IP) of Myc-tagged SpyCas9-sgRNA (162 kDa) or GST-tagged Acr proteins (free-GST, 27 kDa; IIA4, 37 kDa; $IIA16_{Lmo}$, 50 kDa; $IIA17_{Sga}$, 39 kDa; $IIA18_{Sma}$, 48 kDa; and $IIA19_{Ssim}$, 42 kDa). Left: immunoblot probed with anti-Myc (top) and anti-GST (bottom). Dashed lines indicate where the image is cropped to show only the bands corresponding to full-length SpyCas9, see Extended Data Fig. 4c for the uncropped version. Data shown are representative of two independent experiments. Right: schematic of immunoprecipitation from *P. aeruginosa* cells co-expressing SpyCas9 and Acr proteins followed by analysis. **b**, Time courses of target DNA cleavage reactions using SpyCas9 co-immunoprecipitated with AcrIIA proteins from (**a**) and Extended Data Fig. 4b. Representative timepoints are shown at the top of each lane. (L), 1-kb double stranded DNA ladder; (–), DNA template alone. Data shown are representative of two independent experiments. **c**, Immunoprecipitation of GST-tagged Acr proteins (free-GST, 27 kDa; IIA4, 37 kDa; IIA1, 44 kDa; $IIA16_{Lmo}$, 50 kDa; $IIA17_{Sga}$, 39 kDa; $IIA18_{Sma}$, 48 kDa; and $IIA19_{Ssim}$, 42 kDa) from *P. aeruginosa* co-expressing sgRNA-loaded SpyCas9 or ApoSpyCas9 without sgRNA (162 kDa). Immunoblot for Myc-Cas9 (top) or GST-Acr (bottom). Data shown are representative of two independent experiments.

broad-spectrum AcrIIA5 (ref. [29]; Fig. 5a). Furthermore, by titrating the molar ratio of Acr plasmids transfected (Fig. 5b), inhibition with AcrIIA16 was observed even with very low amounts of Acr plasmid, at levels comparable with other 'gold standard' SpyCas9 inhibitors AcrIIA4 and AcrIIA5. The other six AcrIIA17–19 proteins exhibited more modest and inconsistent levels of inhibition, where at least one homologue of each moderately inhibited SpyCas9 (Fig. 5a,b).

Next, because our *Enterococcus* experiments suggested the potential for broad-spectrum inhibition with the reported Acr proteins, we examined the activities of these same 13 Acr proteins against other commonly used type II-A and II-C Cas9 orthologues: SauCas9, NmeCas9, Sth1Cas9, Sth3Cas9, Nme2Cas9 and CjeCas9 (Fig. 5c–f and Extended Data Fig. 5). Interestingly, $AcrIIA16_{Efa}$ inhibited gene editing by all six additional Cas9 proteins to levels comparable with control inhibitors of each specific system (Fig. 5 and Extended Data Fig. 5). Titrations revealed potent inhibition of SauCas9 by $AcrIIA16_{Efa}$, similar to AcrIIA5 (Fig. 5c,d), and $AcrIIA17_{Efa}$ robustly inhibited NmeCas9 (Fig. 5e,f) confirming the

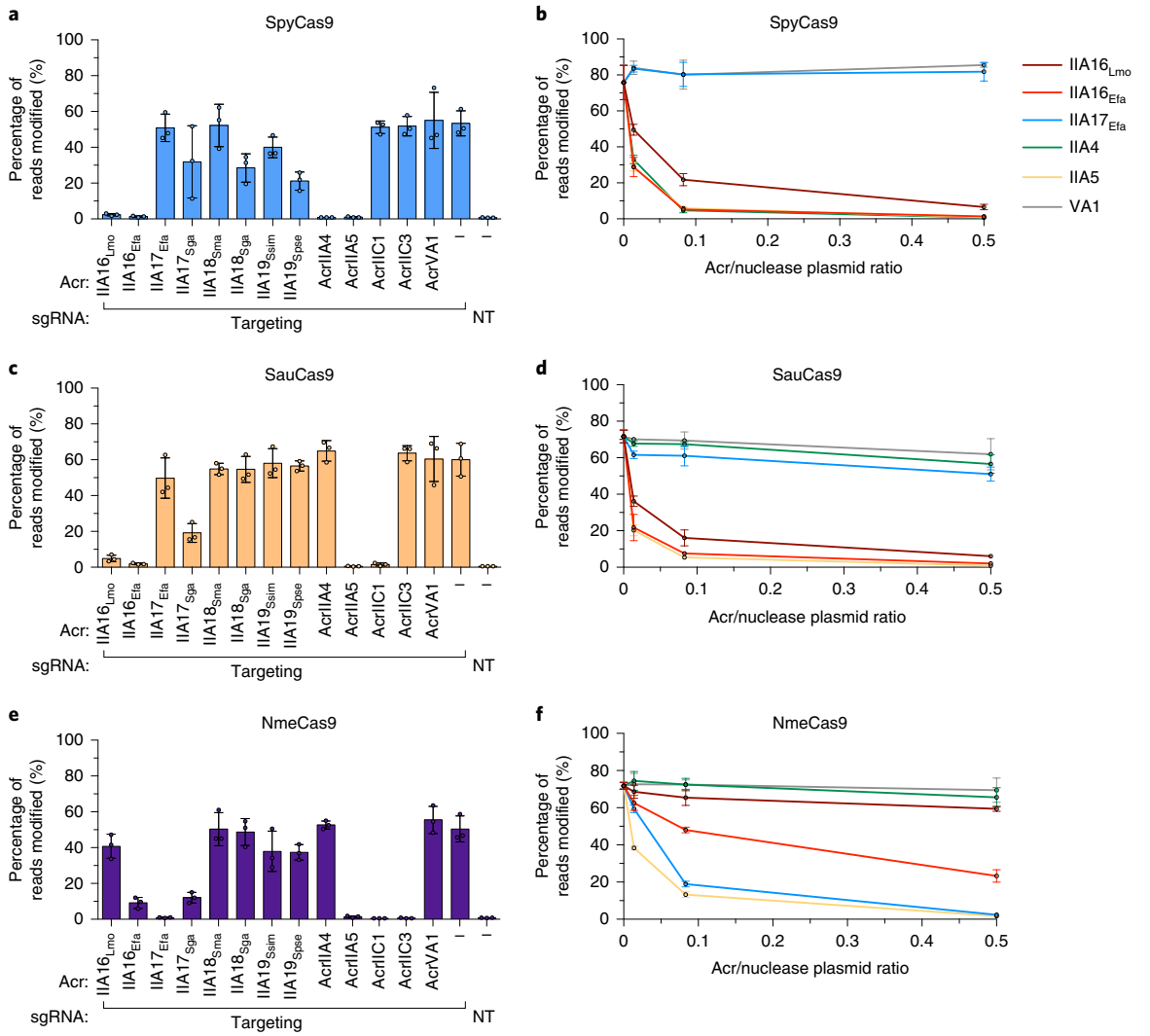

Fig. 5 | Acr-mediated inhibition of Cas9 orthologues during gene editing in human cells. a–f, Reported Acr proteins in this study and from previous work tested for inhibition of genome editing activities of SpyCas9 (**a**,**b**), SauCas9 (**c**,**d**) and NmeCas9 (**e**,**f**). Inhibition is assessed at a fixed Acr/nuclease ratio for all Acr proteins (3/1 for **a**,**c**,**e**) or at various ratios of Acr/nuclease plasmid (0.5/1, 0.083/1 and 0.014/1) for select Acr proteins (**b**,**d**,**f**). Editing efficiencies against endogenous genes in HEK293T cells were assessed by targeted sequencing and quantified as the percentage of reads containing a nuclease-induced alteration; the no-Acr condition contains an enhanced green fluorescent protein expression plasmid; the NT control includes an empty U6 expression plasmid. Percent reads modified are represented as the mean of three biological replicates ± s.d.

broad-spectrum nature of these Acr proteins. Taken together, we observe that the previously unidentified AcrIIA16–19 are found in many MGEs (phages, plasmids and so on) and are capable of inhibiting Cas9 orthologues in different cell backgrounds, including native and heterologous bacterial and human cells.

Discussion

Numerous strategies continue to be developed for the identification of Acrs, with a remarkably diverse range of disclosed inhibition mechanisms[33,34]. Here, we discovered *acr* loci in various MGEs, led initially by gene associations with *acrIIA1* (refs. [19,31]). The *acr* genes reported here are found in diverse MGEs including plasmids, integrative and conjugative elements, prophages, transposons, integrons and other uncharacterized elements. These Cas9 inhibitors protect phage DNA during infection and plasmid DNA during conjugation. AcrIIA16–19 interact with SpyCas9 via distinct binding mechanisms compared with AcrIIA4 and AcrIIA2 to ultimately inhibit target DNA cleavage. Finally, AcrIIA16 and AcrIIA17 displayed potent inhibition of type II-A and II-C Cas9 orthologues, respectively.

It is of high clinical relevance to find *acrIIA* genes in *E. faecalis*, where the spread of antibiotic resistance genes is frequently promoted through plasmid transfer despite the presence of host-encoded CRISPR–Cas systems. This work opens the door to the identification of more *acr* genes in this organism and its relatives. Previous work has shown that multidrug resistant *E. faecalis* strains are more likely to lack CRISPR–Cas9 but can acquire MGEs with protospacer matches due to low levels of Cas9 expression, and tolerate those plasmids transiently[32,35,36]. Our results suggest that these complex interactions have an additional layer and that a state of plasmid self-targeting could be stabilized for some time before potential CRISPR–Cas or spacer loss. We demonstrated that AcrIIA proteins could not only enhance the spread of the antibiotic resistance plasmid that encodes them, but also impair the host's ability to limit the acquisition of other MGEs. Future work on the mechanism and diversity of *acr* genes in *E. faecalis* will be necessary to understand their prevalence and importance in HGT.

The AcrIIA proteins reported in this work appear to modulate sgRNA levels or lengths when co-expressed with sgRNA and Cas9.

In addition, AcrIIA16 can directly impair Cas9 function when exposed to sgRNA and ApoSpyCas9 separately before loading, but not when exposed to loaded RNP in vitro. Further investigation of these Acr proteins in their native host may be required to truly understand their mechanism (that is, where CRISPR RNA (crRNA) and trans-activating crRNA are encoded separately and processing must occur) and direct in vitro interaction mapping coupled with structural analysis is needed.

With the increasing use of CRISPR–Cas systems for various genome editing applications, the discovery and characterization of natural inhibitors that regulate a variety of Cas9 orthologues via different mechanisms remains critical. The broad-spectrum inhibitors AcrIIA16 and IIA17 are attractive as practical regulators of multiple distinct Cas9 proteins. We also observed that AcrIIA5 is a good candidate for broad-spectrum Cas9 inhibition, as reported previously[21,29]. AcrIIC1 also performed well against SauCas9 and NmeCas9; however, it was reported in a previous assay to not inhibit SauCas9 in vitro[37]. The discovery of Acr proteins in organisms with more than one type II-A CRISPR–Cas9 system (for example, *Streptococcus, Listeria* and *Enterococcus*) may lead to the identification of other broad-spectrum inhibitors as there is a selective pressure to inhibit multiple Cas9-based systems. Conjugative elements with a broader host range than phages may face extensive and variable pressure, and thereby are promising for the discovery of uncharacterized *acr* genes and mechanisms.

Methods

Microbes. *Escherichia coli* (DH5α, XL1Blue, NEB 10-beta or NEB turbo) were routinely cultured in lysogeny broth (LB) at 37 °C supplemented with antibiotics at the following concentrations: gentamicin (30 μg ml^{-1}), carbenicillin (100 μg ml^{-1}), kanamycin (25 μg ml^{-1}), chloramphenicol (25 μg ml^{-1}), erythromycin (300 μg ml^{-1}) or tetracycline (10 μg ml^{-1}). *P. aeruginosa* (PAO1) was cultured in LB medium at 37 °C with supplemented antibiotics for plasmid maintenance: gentamicin (50 μg ml^{-1}) or carbenicillin (250 μg ml^{-1}). For maintaining multiple plasmids in the same *P. aeruginosa* strain, antibiotic concentrations were adjusted to 30 μg ml^{-1} gentamicin and 100 μg ml^{-1} carbenicillin. All *E. faecalis* strains (C173, OG1RF, T11RF and T11RFΔCas9) were cultured in brain–heart infusion medium at 37 °C, unless otherwise mentioned. Antibiotics were used in the following concentrations: spectinomycin (500 μg ml^{-1}), streptomycin (500 μg ml^{-1}), rifampicin (50 μg ml^{-1}), fusidic acid (25 μg ml^{-1}), chloramphenicol (15 μg ml^{-1}) or erythromycin (50 μg ml^{-1}).

Cell lines. Human HEK293T cells were obtained from the American Type Culture Collection and authenticated by short tandem repeat profiling. Cells were cultured in DMEM supplemented with 10% heat-inactivated fetal bovine serum and 1% penicillin/streptomycin. Media supernatant from cell cultures was analysed monthly for the absence of mycoplasma using MycoAlert PLUS (Lonza).

Construction of *P. aeruginosa* and *E. faecalis* strains. The *P. aeruginosa* heterologous type II-A system was generated as previously described[30] under 'construction of PAO1::SpyCas9 expression strain' in the Methods section, with sgRNA integrated into the bacterial genome using the mini-CTX2 vector[38] or expressed from multicopy episomal plasmid pMMB67HE-P_{Lac} (where subscripted Lac indicates the promoter is a lactose-inducible promoter or lactose analogue IPTG-inducible promoter) for in vivo assays, and plasmid pHERD30T-P_{Bad} (where subscripted Bad indicates the promoter is an arabinose-inducible promoter) for in vitro assays. All *acr* candidate genes were synthesized as gene fragments (Twist Biosciences) and cloned using Gibson Assembly into plasmids of *P. aeruginosa* vectors pHERD30T or pMMB67HE, and *E. faecalis* vectors pKH12 or pMSP3535 (gifts from K. L. Palmer and G. M. Dunny RRID:Addgene_46886, respectively). Plasmids were electroporated into PAO1 for all *P. aeruginosa* strains[39], and *E. faecalis* strains C173, OG1RF, T11RF and T11RFΔCas9 using previously published protocols[40]. All strains and plasmids constructed and used in this study are listed in Supplementary Table 3a,b.

Bacteriophage plaque assays in *P. aeruginosa*. Plaque assays were performed as previously described[25,30] with sgRNA designed to target *Pseudomonas* phage JBD30. The P_{Lac} promoter driving chromosomally integrated SpyCas9 and sgRNA or pMMB67HE-sgRNA was induced with titrating levels of IPTG (0.1, 1 and 10 mM) and the P_{Bad} promoter driving pHERD30T-*acr* with 0.1% arabinose. One representative plate for each candidate was imaged using the Gel Doc EZ Gel Documentation System (Bio-Rad) and Image Lab software.

Self-genome targeting and CRISPRi assay in *P. aeruginosa*. Strains with chromosomally integrated wild-type SpyCas9 or dCas9 were programmed with pMMB67HE-sgRNA to target the PAO1 chromosomal *phzM* gene promoter in the presence of pHERD30T-*acr*. Cultures were grown overnight in LB supplemented with appropriate antibiotics for plasmid maintenance and 0.1% arabinose to pre-induce anti-CRISPR expression. Overnight cultures were diluted in 1:100 LB supplemented with inducers 0.1% arabinose and IPTG (0.1, 0.25, 1 and 10 mM to titrate CRISPR strength) in a 96-well Costar plate (150 μl per well) for self-targeting survival analysis or glass tubes (3 ml) for CRISPRi, in triplicates. Self-genome targeting was assayed by measuring bacterial growth curves for 16–24 h in a Synergy H1 microplate reader (BioTek, using Gen5 software) at 37 °C with continuous shaking, and data displayed as the mean optical density $(OD)_{600}$ of at least three biological replicates ± s.d. (error bars) as a function of time. For CRISPRi, cells were grown for 20–24 h with continuous shaking. Next, pyocyanin was extracted and quantified as previously described[15]. Data are displayed as the mean OD_{520} of at least three biological replicates ± s.d. (error bars) and representative pictures are shown.

Phylogenetic tree construction. Homologues were identified using one run of iterative PSI-BLASTp and an *e*-value cut off <0.1. The distance tree of results was generated on BLAST using the fast minimum-evolution tree method, 0.85 maximum sequence difference and the Grishin (protein) distance model. Further labels and annotations were performed on FigTree.

Host and MGE distribution prediction. Genomes were first annotated as plasmids or phages and their host class according to the NCBI description. Next, genes adjacent to the specified loci were examined for the presence of phage, plasmid or bacteria chromosomal proteins and identified as signature genes, as listed in Supplementary Table 2. For draft genomes where signature genes cannot be identified, PlasFlow was used to predict putative plasmid elements with a threshold adjusted to 0.5 and Phaster was used to predict putative prophages.

Conjugation assay in *E. faecalis*. Protospacers perfectly matching indicated spacers in CRISPR1 or CRISPR3 array (Fig. 2b) were synthesized as complementary oligonucleotides (Integrated DNA Technologies) and cloned into pKH12 (ref. [32]) to generate the targeted conjugative plasmid. The promoter region of the *acr* loci in *E. faecalis* (nucleotide sequence 350 base pairs (bp) upstream) was synthesized (Twist Bioscience) and cloned upstream of the *acr* genes of the targeted pKH12 conjugative plasmid or pMSP3535. The derivatives of pKH12 were introduced into the C173 donor strain as the transferring plasmid, and pMSP3535 into OG1RF, T11RF or T11RFΔCas9 to pre-express the Acr proteins in recipient cells.

Conjugation mating experiments were performed as previously described[5], except for the following adjustments. Diluted cultures of plasmid-donor and recipient strains were grown to an OD_{600} of 0.9–1.0, after which 100 μl of donor strain was mixed with 900 μl of OG1RF recipient strains or 500 μl of donor with 500 μl of T11RF recipients. Resuspended pellets were plated on Mixed Cellulose Ester filter membranes (Advantec no. A020H047A) on brain–heart infusion agar plates without selection and incubated overnight at 37 °C. The next day, mated cells were collected by washing the filter membrane with 1.5 ml of 1× PBS and tenfold serial dilutions were plated or spotted on brain–heart infusion agar plates supplemented with antibiotics to quantify donor (spectinomycin, streptomycin and chloramphenicol), recipient (rifampicin and fusidic acid, and erythromycin for pMSP353 containing strains) or transconjugant (rifampicin, fusidic acid and chloramphenicol, with erythromycin for pre-expressed Acr strains) populations. Plates were incubated for 48 to 72 h at 30 °C to allow colonies to develop. Plates with 30 to 300 colonies were used to calculate colony forming units per ml and conjugation frequency was determined by dividing the number of transconjugants over donors. For plates with spotted dilutions, the fold reductions in transconjugants were qualitatively derived by examining at least three replicates of each experiment. Plate images were acquired as in Bacteriophage plaque assays in P. aeruginosa and a representative picture is shown.

Expression and purification of anti-CRISPR proteins. N-terminally glutathione *S*-transferase (GST)-tagged Acr proteins were purified from *E.* coli BL21 following a previous protocol[31] under 'Cas9 and anti-CRISPR protein expression and purification' in the Methods section. Lysates were incubated with Glutathione Sepharose (GE 17-0756-05) followed by dialysis by centrifugation into a storage buffer (100 mM Tris-Cl pH 8, 150 mM KCl, 10% glycerol and 1 mM dithiothreitol (DTT)) to remove reduced glutathione used in elution.

Cleavage assays using purified proteins. Lyophilized sgRNA was resuspended in Nuclease-free Duplex buffer following the protocol from Integrated DNA Technologies, and stored frozen at −80 °C or incubated with SpyCas9 (NEB) at room temperature for 15 min to form SpyCas9 RNP. All reactions were carried out in 1× MST buffer (50 mM Tris-Cl pH 7.4, 150 mM NaCl, 20 mM $MgCl_2$, 5 mM DTT, 5% glycerol, 0.05% Tween-20 [v/v]). Then 25 nM SpyCas9 RNP was incubated with 2,500 nM of Acr protein for 10 min at room temperature. For the sgRNA preincubation experiment, 25 nM sgRNA alone was incubated with 2,500 nM Acr protein for 15 min at room temperature, followed by SpyCas9 for 10 min at room temperature to form 25 nM RNP. DNA substrate linearized by NheI digestion was added to a final concentration of 2 nM and the reaction was allowed to cut for 1, 5, 10 and 30 min, and at each time point the reaction was quenched in warm Quench buffer (50 mM EDTA, 0.02% SDS) followed by heating at 95 °C for 10 min. Products were analysed on 1% agarose gel and stained with SYBR Safe.

Table 1 | Summary of anti-CRISPRs reported and inhibition activity

Anti-CRISPR	Strain	Accession number[a]	Inhibits Cas9?[b]	Inhibits SpyCas9 in *P. aeruginosa* heterologous system?[b]	Inhibits EfaCas9 in *E. faecalis* native system?[b]		Inhibits Cas9 orthologues in mammalian cells system?[b]			
					CRISPR1 (Spy-like)	CRISPR3 (Sau-like)	Spy	Sau	Sth1	Nme
IIA16-Lmo	*Listeria monocytogenes*	WP_061665674.1	Yes	Yes	Yes	Yes	Yes	Yes	Yes	No
IIA16-Efa	*Enterococcus faecalis*	WP_025188019.1	Yes	ND	ND	ND	Yes	Yes	Yes	Yes
IIA17-Efa	*Enterococcus faecalis*	WP_002401839.1	Yes	Yes	Yes	Yes	No	No	No	Yes
IIA17-Sga	*Streptococcus gallolyticus*	WP_074626943.1	Yes	Yes	Yes	Yes	Yes	Yes	No	Yes
IIA18-Sma	*Streptococcus macedonicus*	WP_099390844.1	Yes	Yes	ND	ND	No	No	No	No
IIA18-Sga	*Streptococcus gallolyticus*	WP_074627086.1	Yes	ND	ND	ND	Yes	No	No	No
IIA19-Ssim	*Staphylococcus simulans*	WP_107591702.1	Yes	Yes	Yes	Yes	No	No	No	No
IIA19-Spse	*Staphylococcus pseudintermedius*	WP_100006909.1	Yes	ND	ND	ND	Yes	No	No	No

[a]List of accession numbers for AcrIIA16–19 proteins reported in this study. [b]Summary of their inhibition activity against Cas9 orthologues. ND, not determined.

Co-immunoprecipitation of SpyCas9-3×Myc and GST-Acr. In the *P. aeruginosa* PAO1 strain, chromosomally integrated SpyCas9 and plasmid-encoded pHERD30T-sgRNA for guide-loaded Cas9 or empty vector for apoCas9 were expressed off the P_{Bad} promoter, and pMMB67HE-GST-AcrIIA were expressed off the P_{Lac} promoter. Saturated overnight cultures were diluted 1:100 the next morning in a total volume of 50 ml, induced with 0.3% arabinose and 1 mM IPTG at an OD_{600} of 0.3–0.4 and harvested at an OD_{600} of 1.8–2.0 by centrifugation at 6,000*g* for 10 min at 4 °C. Cell pellets were flash frozen on dry ice, resuspended in 1 ml lysis buffer (50 mM Tris-Cl pH 7.4, 150 mM NaCl, 20 mM $MgCl_2$, 0.5% NP40, 5% glycerol [v/v], 5 mM DTT and 1 mM PMSF), lysed by sonication (a 20 s pulse for 4 cycles with cooling on ice between cycles), and lysates were clarified by centrifugation at 14,000*g* for 10 min at 4 °C. For input samples, 10-µl lysates were added in 3× volume of the 4× Laemmli sample buffer. Using a magnetic stand, Anti-c-Myc Magnetic Beads no. 88842 or Gluthathione Magnetic Agarose Beads no. 78601 (Thermo Fisher Scientific) were prewashed with 1 ml of cold wash buffer (50 mM Tris-Cl pH 7.4, 150 mM NaCl, 20 mM $MgCl_2$), and the remaining lysate was added to the bead slurry in a volume ratio of 20:1 for Myc or 40:1 for GST followed by overnight incubation at 4 °C with end-over-end rotation. Beads were washed five times using a magnetic stand at room temperature with 1 ml of cold wash buffer with addition of 5 mM DTT, gradually decreasing the concentrations of detergent NP40 (0.5%, 0.05%, 0.01%, 0.005%, 0) and glycerol (5%, 0.5%, 0.05%, 0.005%, 0). Bead-bound proteins were resuspended in 100 µl of final wash buffer without detergent and glycerol. For analysis, 10 µl of bead-bound proteins were added to an equal volume of 4× Laemmli sample buffer. Samples were analysed on 4–20% SDS–PAGE gel and stained with Coomassie (Bio-Safe Coomassie Stain, Bio-Rad).

Immunoblotting. Protein samples were separated by SDS–PAGE using 4–20% gel (Mini-PROTEAN TGX Precast Gels, Bio-Rad) and transferred in 1× Tris-glycine buffer (Bio-Rad) with 20% methanol onto a 0.2-µm Immun-Blot PVDF Membrane (Bio-Rad). Blots were probed with the following antibodies diluted 1:5,000 in 1× TBS-T containing 5% non-fat dry milk: mouse anti-Myc (Cell Signaling Technology no. 2276, RRID:AB_331783), rabbit anti-GST (Cell Signaling Technology no. 2625, RRID:AB_490796), horseradish peroxidase-conjugated goat anti-mouse Immunoglobulin-G (Santa Cruz Biotechnology no. sc-2005, RRID:AB_631736) and horseradish peroxidase-conjugated goat anti-rabbit Immunoglobulin-G (Bio-Rad no. 170-6515, RRID:AB_11125142). Blots were developed using Clarity ECL Western Blotting Substrate (Bio-Rad), and chemiluminescence was detected on an Azure c400 Biosystems Imager.

Cleavage assays using SpyCas9-3×Myc tagged pulldowns. DNA substrate linearized by NheI digestion was added into bead-bound protein slurry to a final concentration of 1.5 nM and the reaction was allowed to react for 1, 5, 10 and 30 min in the thermomixer at 25 °C with gentle shaking at 1,000 r.p.m. At each time point, the reaction was quenched in warm Quench buffer (50 mM EDTA, 0.02% SDS), followed by heating at 95 °C for 10 min. Products were analysed on 1% agarose gels stained with SYBR Safe.

RNA extraction. Chromosomally integrated SpyCas9 and pHERD30T-sgRNA were expressed off the P_{Bad} promoter, and pMMB67HE-GST-AcrIIA expressed off the P_{Lac} promoter in *P. aeruginosa* PAO1 strain. Saturated overnight cultures were diluted 1:100 the next morning in a total volume of 10 ml of LB containing the inducers 0.1% arabinose and 1 mM IPTG and harvested at an OD_{600} of 0.8–0.9 by centrifugation at 6,000*g* for 10 min at 4 °C. Total RNA was extracted using TRIzol Max Bacterial RNA Isolation Kit (Life Technologies 16096-020), and treated with DNase I (Turbo DNA-free kit AM1907 from Life Technologies) according to the manufacturer's protocol. The concentration of RNA in each sample was further normalized following spectrophotometry measurements using NanoDrop.

Northern blot analysis. Northern blot was carried out as previously described[12], with exceptions described as follows. The radiolabelled probe was generated by amplifying a fragment containing the sgRNA constructed from the pHERD30T plasmid with primers CCAAACCGGTAACCCCGCTTA and GATTAAGTTGGGTAACGCCAGGGTTTTC, cleaning the PCR product (DNA Clean and Concentrator Kit D4034 from Zymo Research), labelling 200 ng of the clean product with anti-32P deoxycytidine triphosphate (dCTP) using DNA Polymerase I Klenow Fragment (NEB M0210L) and purification using G25 columns (GE Healthcare) to remove unincorporated nucleotides. Then 5 ug of total RNA extracts were loaded using 2× RNA Loading Dye (NEB B0363S) onto a 15% denaturing gel (Mini-PROTEAN TBE-Urea Gel from Bio-Rad) and separated by electrophoresis. RNA was transferred onto Hybond-N+ membrane (GE Healthcare RPN303B) via a semi-dry apparatus (Trans-Blot Turbo Transfer System from Bio-Rad) at 200 mA for 1 h and then crosslinked with a 10 mJ ultraviolet burst over 30 s (Stratagene). The membrane was blocked with prehybridization buffer (50% formamide, 5× Denhardts solution and 6× SSC) containing 100 µg ml^{-1} salmon sperm DNA at 42 °C for 1.5 h with rotation, followed by hybridization with a radiolabelled probe at 42 °C overnight with rotation. The blot was washed with wash solution 1 (2× SSC and 1% SDS), twice for 10 min at 25 °C, twice for 30 min at 65 °C and wash solution 2 (0.2× SSC and 0.1% SDS) once for 10 min at 25 °C. Blots were developed using a phosphor screen and Typhoon imager.

Plasmid for human cell experiments. Descriptions of all plasmids used for expression of nucleases and Acr proteins in human cells, sgRNA/crRNA entry vectors and all sgRNA/crRNA target sequences are listed in Supplementary Table 4. U6 promoter sgRNA and crRNA expression plasmids were generated by annealing and ligating oligonucleotide duplexes into BsmBI-digested entry vectors (Supplementary Table 4b). Human codon optimized Acr constructs containing a C-terminal SV40 nuclear localization signal were cloned into NotI/AgeI of Addgene plasmid ID 43861. New human expression plasmids described in this study have been deposited with Addgene (Supplementary Table 4a).

Human cell culture and transfection. HEK293T cells were seeded at 2×10^4 cells per well in 96-well plates approximately 20 h before transfection. Each transfection reaction consisted of 1.25 µl of TransIT-X2 (Mirus Bio) with 70 ng of nuclease, 30 ng of sgRNA/crRNA and 110 ng of anti-CRISPR expression plasmids in a final volume of 20 µl otherwise containing Opti-MEM (Thermo Fisher Scientific). For control conditions containing no Acr plasmid, 110 ng of a pCMV-enhanced green fluorescent protein plasmid was utilized; for non-targeting sgRNA/crRNA conditions, 30 ng of an empty U6 promoter plasmid was used. For titration experiments, cells were transfected with 70 ng of nuclease, 30 ng sgRNA/crRNA, varying amounts of acr expression and DNA stuffer plasmids totalling 96.5 ng (0.5 ng Acr with 96 ng stuffer; 2.75 ng acr with 93.75 ng stuffer; 16 ng acr with 80.5 ng stuffer), and 1.17 µl of TransIT-X2 (Mirus Bio) in 20 µl of Opti-MEM. DNA stuffer plasmids were an orthogonal and incompatible pCAG-MbCas12a expression plasmid. Genomic DNA was harvested approximately 72 h post-transfection by suspending cells in 100 µl of lysis buffer (20 mM HEPES pH 7.5, 100 mM KCl, 5 mM $MgCl_2$, 5% glycerol, 25 mM DTT, 0.1% Triton X-100 and 30 ng $µl^{-1}$ Proteinase K (NEB)), followed by incubation at 65 °C for 6 min and 98 °C for 2 min. All experiments were performed with at least three independent biological replicates.

Assessment of genome editing in human cells. Genome modification was measured by next-generation sequencing using a two-step PCR-based Illumina library construction method. Briefly, genomic regions were initially amplified using Q5 High-Fidelity DNA Polymerase (NEB), human cell lysate containing ~100 ng of genomic DNA and gene-specific round one primers (Supplementary Table 4c). PCR products were purified using paramagnetic beads as previously

described[41] and diluted 1:100 to serve as template for a second round of PCR using Q5 High-Fidelity Polymerase and primers encoding Illumina barcodes and adaptor sequences (Supplementary Table 4c). PCR products were purified before quantification (via Qiagen QIAxcel electrophoresis), normalization and pooling. Final libraries were quantified by qPCR (Illumina Library qPCR Quantification Kit, KAPA Biosystems) and sequenced on a MiSeq sequencer using a 300-cycle v2 kit (Illumina). Genome editing activities were determined from the sequencing data using CRISPResso2 (ref. [42]) with commands -min_reads_to_use_region 100, -w 10, and for certain sequencing data sets -ignore_substitutions.

Reporting Summary. Further information on research design is available in the Nature Research Reporting Summary linked to this article.

Data availability

All data generated or analysed during this study are included in this published article and its Extended Data, Source Data and Supplementary Information files. All relevant accession codes are available in Table 1.

Received: 24 October 2019; Accepted: 14 February 2020;
Published online: 26 March 2020

References

1. Palmer, K. L., Kos, V. N. & Gilmore, M. S. Horizontal gene transfer and the genomics of enterococcal antibiotic resistance. *Curr. Opin. Microbiol.* **13**, 632–639 (2010).
2. Waldor, M. K. & Mekalanos, J. J. Lysogenic conversion by a filamentous phage encoding cholera toxin. *Science* **272**, 1910–1914 (1996).
3. Koonin, E. V. Viruses and mobile elements as drivers of evolutionary transitions. *Philos. Trans. R. Soc. Lond. B* **371**, 20150442 (2016).
4. Labrie, S. J., Samson, J. E. & Moineau, S. Bacteriophage resistance mechanisms. *Nat. Rev. Microbiol.* **8**, 317–327 (2010).
5. PriceV. J., Huo W., Sharifi A. & Palmer K. L. CRISPR-cas and restriction-modification act additively against conjugative antibiotic resistance plasmid transfer in enterococcus faecalis. *mSphere* **1**, e00064-16 (2016).
6. Edgar, R. & Qimron, U. The *Escherichia coli* CRISPR system protects from λ lysogenization, lysogens, and prophage induction. *J. Bacteriol.* **192**, 6291–6294 (2010).
7. Zhang, Y. et al. Processing-independent CRISPR RNAs limit natural transformation in *Neisseria meningitidis*. *Mol. Cell* **50**, 488–503 (2013).
8. Makarova, K. S. et al. An updated evolutionary classification of CRISPR–Cas systems. *Nat. Rev. Microbiol.* **13**, 722–736 (2015).
9. Garneau, J. E. et al. The CRISPR/cas bacterial immune system cleaves bacteriophage and plasmid DNA. *Nature* **468**, 67–71 (2010).
10. Clark, D. P. & Pazdernik, N. J. in *Molecular Biology* 2nd edn, Ch. e26 (Elsevier, 2013).
11. Casjens, S. Prophages and bacterial genomics: what have we learned so far? *Mol. Microbiol.* **49**, 277–300 (2003).
12. Bondy-Denomy, J., Pawluk, A., Maxwell, K. L. & Davidson, A. R. Bacteriophage genes that inactivate the CRISPR/Cas bacterial immune system. *Nature* **493**, 429–432 (2013).
13. Zhu, Y. et al. Diverse mechanisms of CRISPR-Cas9 inhibition by type IIC Anti-CRISPR proteins. *Mol. Cell* **74**, 296–309 (2019).
14. Thavalingam, A. et al. Inhibition of CRISPR–Cas9 ribonucleoprotein complex assembly by anti-CRISPR AcrIIC2. *Nat. Commun.* **10**, 2806 (2019).
15. Bondy-Denomy, J. et al. Multiple mechanisms for CRISPR–Cas inhibition by anti-CRISPR proteins. *Nature* **526**, 136–139 (2015).
16. Harrington, L. B. et al. A broad-spectrum inhibitor of CRISPR-Cas9. *Cell* **170**, 1224–1233 (2017).
17. Dong, L. et al. An anti-CRISPR protein disables type V Cas12a by acetylation. *Nat. Struct. Mol. Biol.* **26**, 308–314 (2019).
18. Knott, G. J. et al. Broad-spectrum enzymatic inhibition of CRISPR–Cas12a. *Nat. Struct. Mol. Biol.* **26**, 315–321 (2019).
19. Rauch, B. J. et al. Inhibition of CRISPR-Cas9 with bacteriophage proteins. *Cell* **168**, 150–158 (2017).
20. Hynes, A. P. et al. An anti-CRISPR from a virulent streptococcal phage inhibits *Streptococcus pyogenes* Cas9. *Nat. Microbiol.* **2**, 1374–1380 (2017).
21. Hynes, A. P. et al. Widespread anti-CRISPR proteins in virulent bacteriophages inhibit a range of Cas9 proteins. *Nat. Commun.* **9**, 2919 (2018).
22. Uribe, R. V. et al. Discovery and characterization of Cas9 inhibitors disseminated across seven bacterial phyla. *Cell Host Microbe* **25**, 233–241 (2019).
23. Forsberg, K. J. et al. Functional metagenomics-guided discovery of potent cas9 inhibitors in the human microbiome. *eLife* **8**, e46540 (2019).
24. Pawluk, A. et al. Naturally occurring off-switches for CRISPR-Cas9. *Cell* **167**, 1829–1838 (2016).
25. Jiang, F. et al. Temperature-responsive competitive inhibition of CRISPR-Cas9. *Mol. Cell* **73**, 601–610 (2019).
26. Liu, L., Yin, M., Wang, M. & Wang, Y. Phage AcrIIA2 DNA mimicry: structural basis of the CRISPR and anti-CRISPR arms race. *Mol. Cell* **73**, 611–620 (2019).
27. Dong, D. et al. Structural basis of CRISPR–SpyCas9 inhibition by an anti-CRISPR protein. *Nature* **546**, 436–439 (2017).
28. Shin, J. et al. Disabling Cas9 by an anti-CRISPR DNA mimic. *Sci. Adv.* **3**, e1701620 (2017).
29. Garcia, B. et al. Anti-CRISPR AcrIIA5 potently inhibits all Cas9 homologs used for genome editing. *Cell Rep.* **29**, 1739–1746 (2019).
30. Borges, A. L. et al. Bacteriophage cooperation suppresses CRISPR-Cas3 and Cas9 Immunity. *Cell* **174**, 917–925 (2018).
31. Osuna, B. A. et al. Listeria phages induce Cas9 degradation to protect lysogenic genomes. Preprint at https://doi.org/10.1101/787200 (2019).
32. Hullahalli, K., Rodrigues, M. & Palmer, K. L. Exploiting CRISPR-Cas to manipulate Enterococcus faecalis populations. *eLife* **6**, e26664 (2017).
33. Trasanidou, D. et al. Keeping crispr in check: diverse mechanisms of phage-encoded anti-crisprs. *FEMS Microbiol. Lett.* **366**, 1–14 (2019).
34. Zhang, F., Song, G. & Tian, Y. Anti-CRISPRs: the natural inhibitors for CRISPR-Cas systems. *Anim. Model. Exp. Med.* **2**, 69–75 (2019).
35. PalmerK. L. & GilmoreM. S. Multidrug-resistant enterococci lack CRISPR-cas. *mBio* **1**, e00227-10 (2010).
36. Hullahalli, K., Rodrigues, M., Nguyen, U. T. & Palmer, K. An attenuated CRISPR-cas system in enterococcus faecalis permits DNA acquisition. *mBio* **9**, e00414-18 (2018).
37. Seamon, K. J., Light, Y. K., Saada, E. A., Schoeniger, J. S. & Harmon, B. Versatile high-throughput fluorescence assay for monitoring Cas9 activity. *Anal. Chem.* **90**, 6913–6921 (2018).
38. Hoang, T. T., Kutchma, A. J., Becher, A. & Schweizer, H. P. Integration-proficient plasmids for *Pseudomonas aeruginosa*: site-specific integration and use for engineering of reporter and expression strains. *Plasmid* **43**, 59–72 (2000).
39. Choi, K. H., Kumar, A. & Schweizer, H. P. A 10-min method for preparation of highly electrocompetent *Pseudomonas aeruginosa* cells: application for DNA fragment transfer between chromosomes and plasmid transformation. *J. Microbiol. Methods* **64**, 391–397 (2006).
40. Bhardwaj, P., Ziegler, E. & Palmer, K. L. Chlorhexidine induces VanA-type Vancomycin resistance genes in enterococci. *Antimicrob. Agents Chemother.* **60**, 2209–2221 (2016).
41. Kleinstiver, B. P. et al. Engineered CRISPR–Cas12a variants with increased activities and improved targeting ranges for gene, epigenetic and base editing. *Nat. Biotechnol.* **37**, 276–282 (2019).
42. Clement, K. et al. CRISPResso2 provides accurate and rapid genome editing sequence analysis. *Nat. Biotechnol.* **37**, 224–226 (2019).

Acknowledgements

We thank K. L. Palmer (UT Dallas) and G. M. Dunny (University of Minnesota) for providing all *E. faecalis* strains, vector and protocols. We thank M. Johnson for his assistance in executing PlasFlow, N. Marino for her profound wisdom and comedic wit, and all members of the Bondy-Denomy Lab for their continuous support and thoughtful discussions contributing to this study. Bondy-Denomy Lab was supported by the UCSF Program for Breakthrough Biomedical Research funded in part by the Sandler Foundation, the Searle Fellowship, the Vallee Foundation, an NIH Director's Early Independence Award No. DP5-OD021344, and NIH grant no. R01GM127489. Research in the Kleinstiver Lab is supported by NIH grant no. R00-CA218870, an A.S.G.C.T. Career Development Award and the Margaret Q. Landenberger Research Foundation.

Author contributions

C.M. and J.B.-D. conceived and designed the study. C.M. conducted bioinformatic, bacterial and biochemical experiments. K.A.C. performed human cell experiments. B.A.O. and R.P.-R. assisted with experimental design. B.P.K and J.B.-D. supervised experiments. C.M. and J.B.-D. wrote the manuscript with input from all authors.

Competing interests

J.B.-D. is a scientific advisory board member of SNIPR Biome and Excision Biotherapeutics, and a scientific advisory board member and co-founder of Acrigen Biosciences. B.P.K. is an inventor on various patents and patent applications that describe gene editing and epigenetic editing technologies, is a consultant for Avectas Inc. and an advisor for Acrigen Biosciences.

Additional information

Extended data is available for this paper at https://doi.org/10.1038/s41564-020-0692-2.

Supplementary information is available for this paper at https://doi.org/10.1038/s41564-020-0692-2.

Correspondence and requests for materials should be addressed to J.B.-D.

Reprints and permissions information is available at www.nature.com/reprints.

Publisher's note Springer Nature remains neutral with regard to jurisdictional claims in published maps and institutional affiliations.

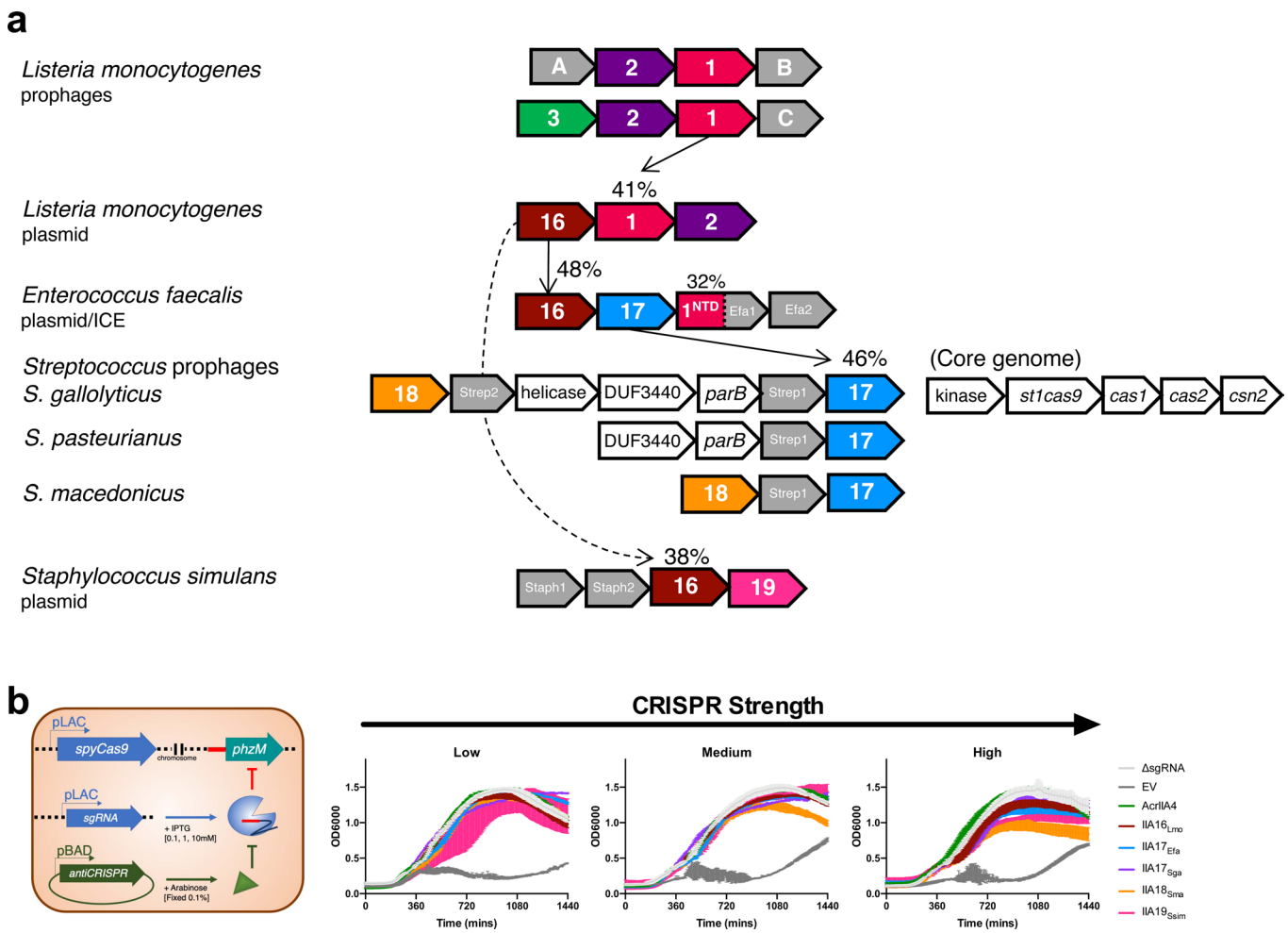

Extended Data Fig. 1 | Schematic of *acr* loci and lethal self-genome cleavage assay. a, Full schematic of *acr* loci with relevant neighboring genes displayed. **b**, Schematic of SpyCas9 in *P. aeruginosa* programmed to cause lethal self-genome cleavage to assess bacterial survival in the presence of AcrIIA proteins. CRISPR strength is determined by titrating levels of IPTG, which induces expression of sgRNA targeting the chromosomal *phzM* gene from a multicopy plasmid. OD600 measurements are represented as the mean of three biological replicates ± SD.

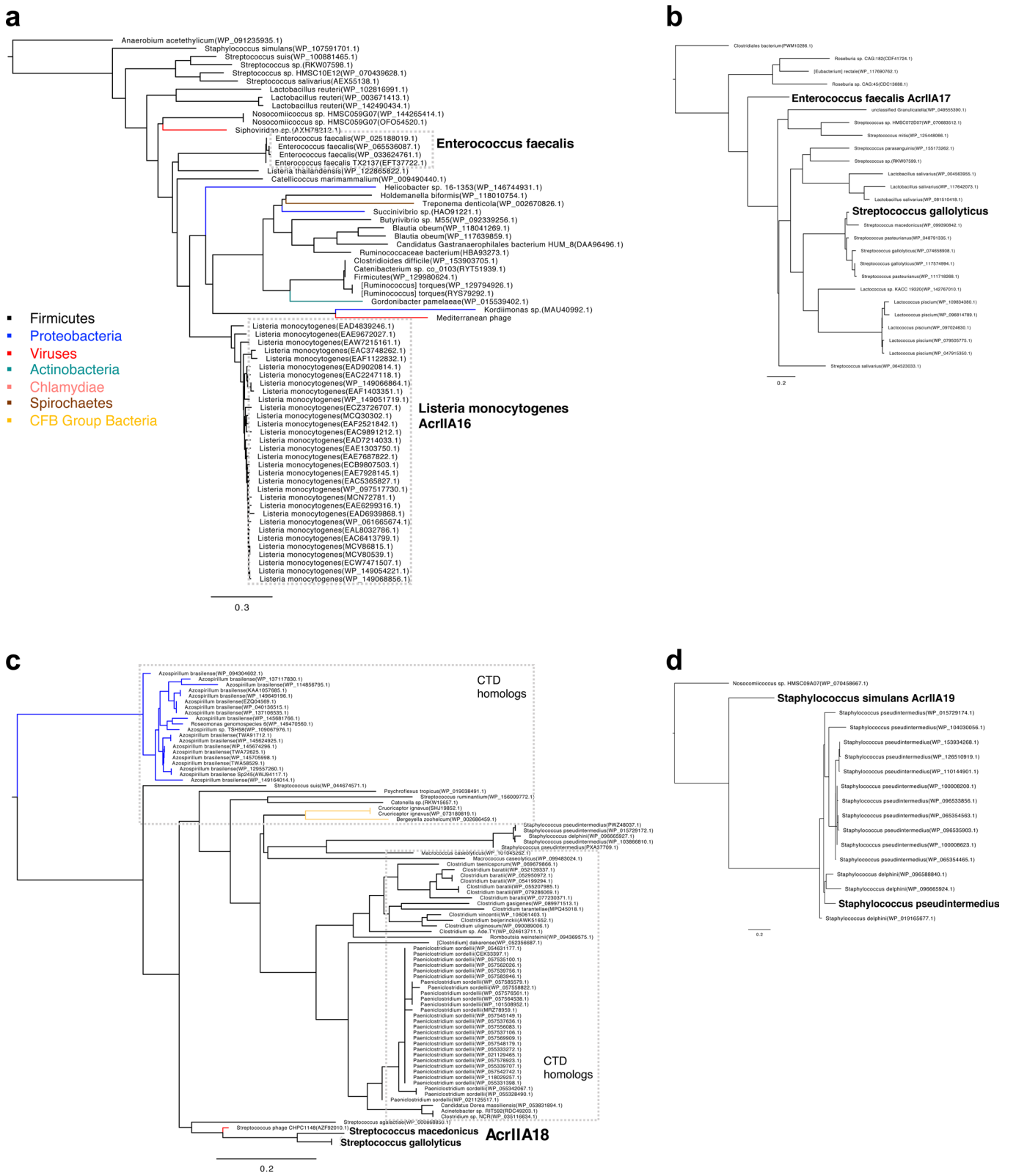

Extended Data Fig. 2 | Anti-CRISPR distribution in integrative mobile genetic elements across bacterial taxa. Phylogenetic analysis based on *acrIIA16–19* homologs (panels **a** to **d**, respectively) reconstructed from a midpoint rooted minimum-evolution of full length protein sequences identified following an iterative PSI-BLASTp search, see methods for details. Number of genomes included to construct each tree for *acrIIA16–19* are seventy, twenty-six, eighty-four and seventeen respectively. Branches are labeled with species name and colored according to species class (see legend). Species for which AcrIIA homologs have been tested in this study are shown in bold.

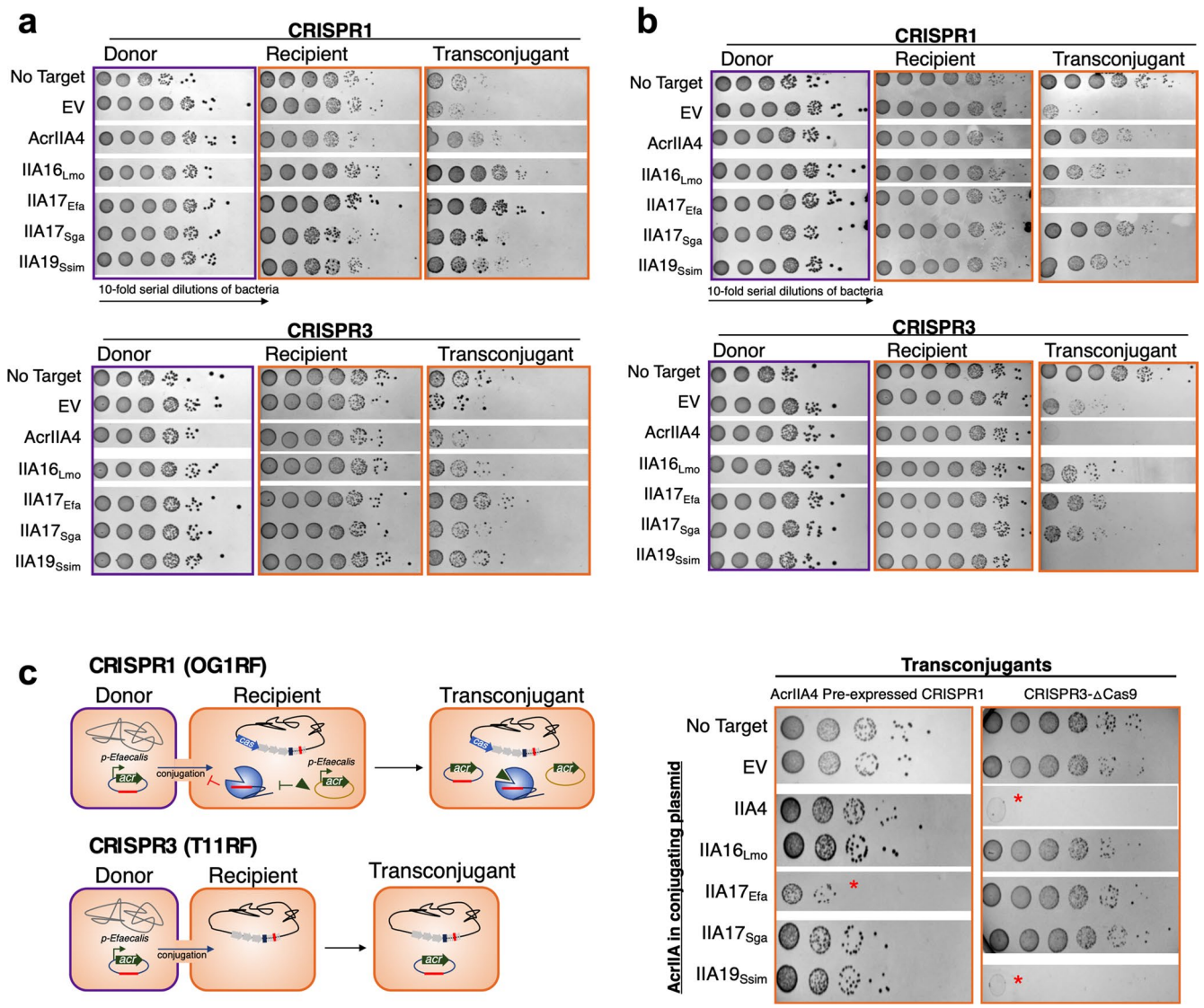

Extended Data Fig. 3 | AcrIIA enhance conjugation-mediated horizontal gene transfer in *E. faecalis*, related to Fig. 2. a, b. Mating outcomes during plasmid conjugation of a targeted plasmid from donor to recipient cells where indicated *acrIIA* genes are **(a)** pre-expressed in recipient cells, or **(b)** encoded on conjugating plasmid. Data displayed as 10-fold colony serial dilution spots of donor, recipient or transconjugant cells on selective antibiotic plates. Mating assays were performed in biological triplicate and produced similar outcomes. **c**, Schematic of *E. faecalis* conjugation of protospacer and *acrIIA*-bearing plasmid transferring into CRISPR-defective recipients. For CRISPR1, the *bona fide* AcrIIA4 is utilized to suppress CRISPR targeting, and a ΔCas9 strain from previously reported work is used for CRISPR3 (Price et al.,[5]). Red * denotes plasmids that have lost conjugation ability. Mating assays were performed in biological duplicate or triplicate and produced similar outcomes.

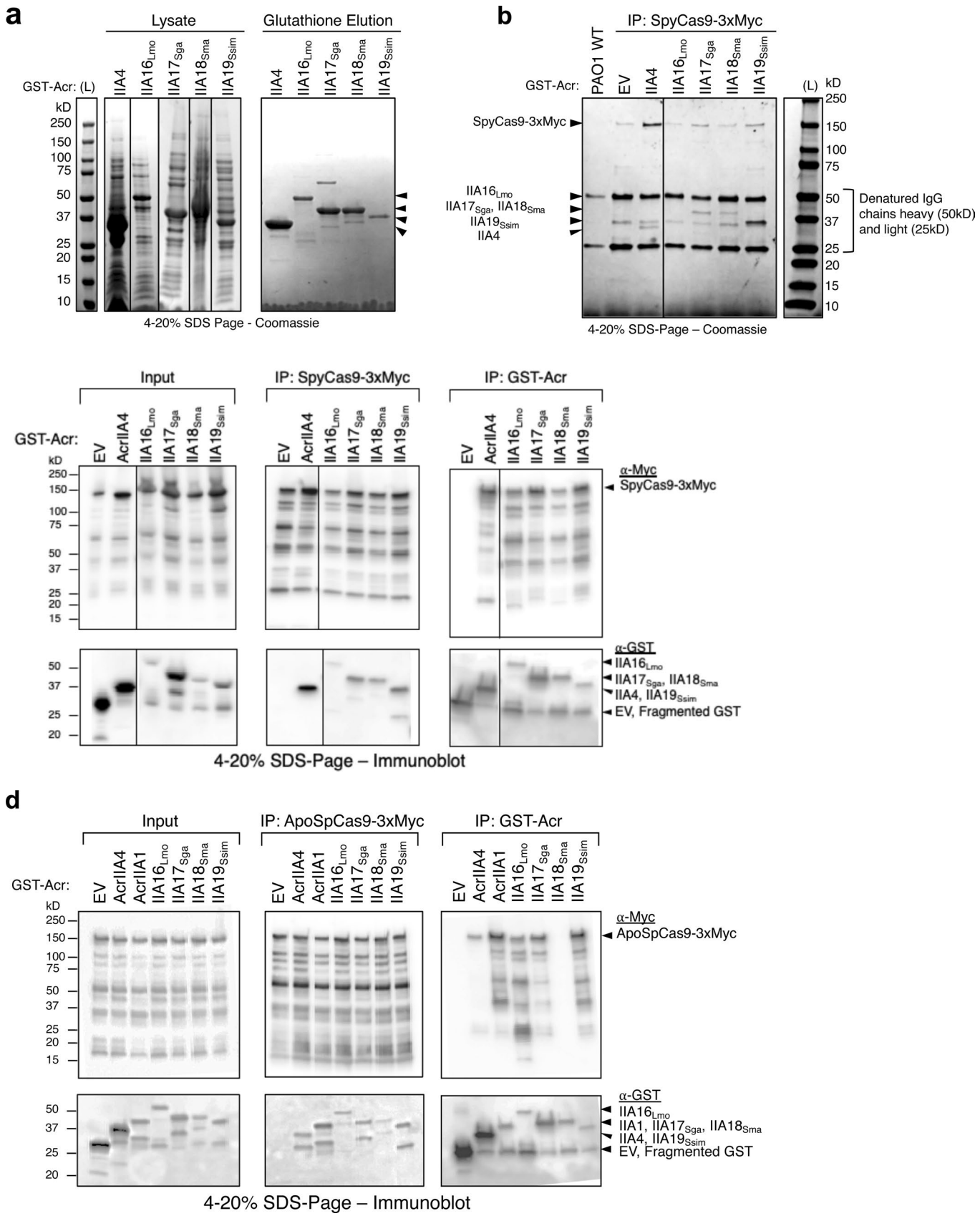

Extended Data Fig. 4 | See next page for caption.

Extended Data Fig. 4 | AcrIIA16–19 biochemical analysis, related to Figs. 3 and 4. a, Coomassie-stained polyacrylamide gel showing GST-tagged AcrIIA proteins (IIA4 37kD, IIA16$_{Lmo}$ 50kD, IIA17$_{Sga}$ 39kD, IIA18$_{Sma}$ 48kD and IIA19$_{Ssim}$ 42kD) purified from *E. coli* by elution from Glutathione Sepharose columns. Visible bands at different sizes are co-purifying proteins from *E. coli*. Data shown are representative of two independent experiments. **b**, Coomassie-stained polyacrylamide gel showing co-immunoprecipitation of Acr proteins with Myc-tagged sgRNA-bound SpyCas9 pulled down from *P. aeruginosa*. Data shown are representative of two independent experiments. **c, d**, Uncropped versions of both Myc and GST pulldowns from Fig. 4a and **c**, displaying all fragments of (**c**) sgRNA-bound SpyCas9, or (**d**) Apo- SpyCas9 without sgRNA present. Data shown are representative of two independent experiments.

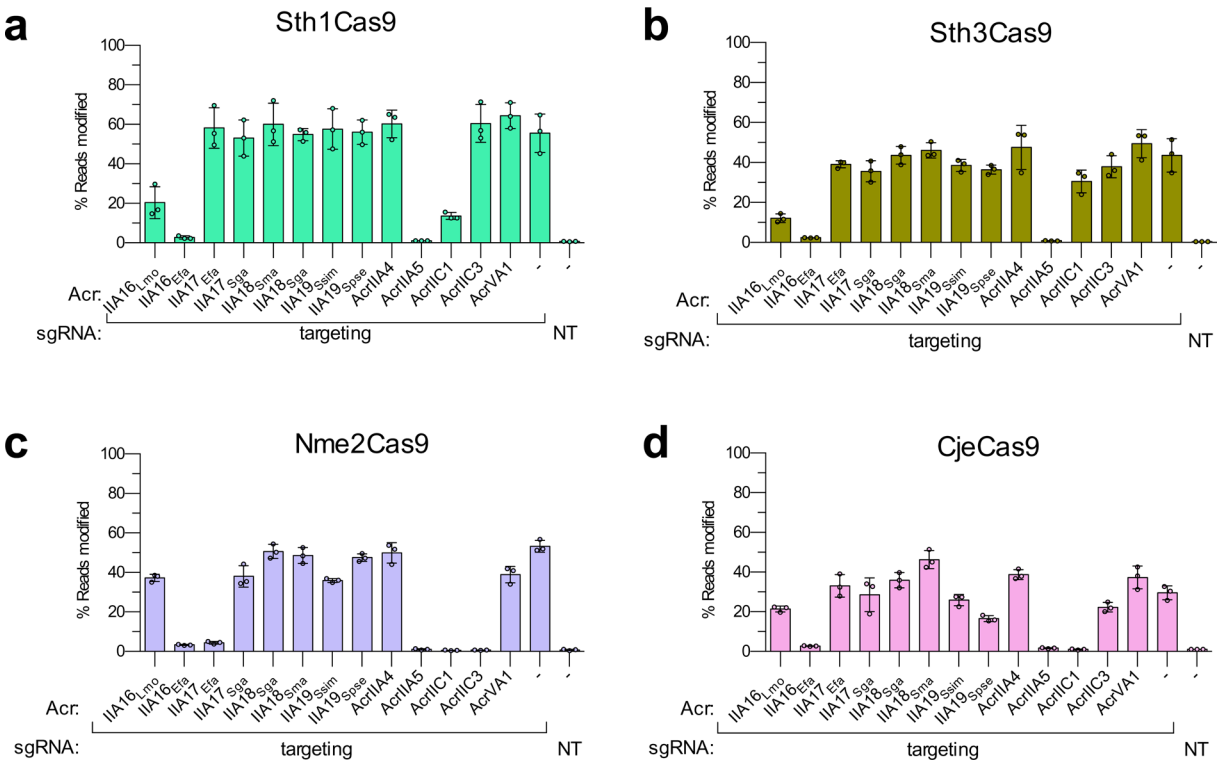

Extended Data Fig. 5 | Acr inhibition activity in human cells tested against different Cas9 orthologs, related to Fig. 5. Reported Acr proteins in this study and from previous works tested for inhibition of genome editing activities of Sth1Cas9, Sth3Cas9, Nme2Cas9 and CjeCas9 (**a-d**, respectively). Editing efficiencies against endogenous genes in HEK 293 T cells were assessed by targeted sequencing and quantified as the percentage of reads containing a nuclease-induced alteration; the no-Acr condition contains an EGFP expression plasmid; the NT control includes an empty U6 expression plasmid. Percent reads modified are represented as the mean of three biological replicates ± SD.

nature research

Corresponding author(s): Joseph Bondy-Denomy

Last updated by author(s): Jan 30, 2020

Reporting Summary

Nature Research wishes to improve the reproducibility of the work that we publish. This form provides structure for consistency and transparency in reporting. For further information on Nature Research policies, see Authors & Referees and the Editorial Policy Checklist.

Statistics

For all statistical analyses, confirm that the following items are present in the figure legend, table legend, main text, or Methods section.

n/a	Confirmed	
☐	☒	The exact sample size (*n*) for each experimental group/condition, given as a discrete number and unit of measurement
☐	☒	A statement on whether measurements were taken from distinct samples or whether the same sample was measured repeatedly
☒	☐	The statistical test(s) used AND whether they are one- or two-sided *Only common tests should be described solely by name; describe more complex techniques in the Methods section.*
☒	☐	A description of all covariates tested
☒	☐	A description of any assumptions or corrections, such as tests of normality and adjustment for multiple comparisons
☐	☒	A full description of the statistical parameters including central tendency (e.g. means) or other basic estimates (e.g. regression coefficient) AND variation (e.g. standard deviation) or associated estimates of uncertainty (e.g. confidence intervals)
☒	☐	For null hypothesis testing, the test statistic (e.g. *F*, *t*, *r*) with confidence intervals, effect sizes, degrees of freedom and *P* value noted *Give P values as exact values whenever suitable.*
☒	☐	For Bayesian analysis, information on the choice of priors and Markov chain Monte Carlo settings
☒	☐	For hierarchical and complex designs, identification of the appropriate level for tests and full reporting of outcomes
☒	☐	Estimates of effect sizes (e.g. Cohen's *d*, Pearson's *r*), indicating how they were calculated

Our web collection on statistics for biologists contains articles on many of the points above.

Software and code

Policy information about availability of computer code

Data collection	Images were taken using Azure Biosystems 2015 cSeries Version 1.6.15.1030 and Image Lab Version 6.0.1 build 34 Standard Edition, bacteria growth curves were collected using Gen5 3.05.11, next-generation sequencing runs to assess genome editing efficiencies were performed using a MiSeq sequencer (Illumina)
Data analysis	Data were analyzed using Microsoft Excel Version 16.30, CRISPResso2 (https://github.com/lucapinello/CRISPResso) and plotted using GraphPad Prism 6.0 or 8.2.1. Phylogenetic tree analyses were performed using FigTree v1.4.4

For manuscripts utilizing custom algorithms or software that are central to the research but not yet described in published literature, software must be made available to editors/reviewers. We strongly encourage code deposition in a community repository (e.g. GitHub). See the Nature Research guidelines for submitting code & software for further information.

Data

Policy information about availability of data

All manuscripts must include a data availability statement. This statement should provide the following information, where applicable:

- Accession codes, unique identifiers, or web links for publicly available datasets
- A list of figures that have associated raw data
- A description of any restrictions on data availability

This study is not associated with the generation of new datasets

Field-specific reporting

Please select the one below that is the best fit for your research. If you are not sure, read the appropriate sections before making your selection.

☒ Life sciences ☐ Behavioural & social sciences ☐ Ecological, evolutionary & environmental sciences

For a reference copy of the document with all sections, see nature.com/documents/nr-reporting-summary-flat.pdf

Life sciences study design

All studies must disclose on these points even when the disclosure is negative.

Sample size	No sample size calculation was performed to determine sample size. Sample sizes of two or three biological replicates are standard for the types of experiment conducted in this study, as in the field of molecular microbiology
Data exclusions	For Fig 1c and Extended Data 1b, only two and three induction levels respectively were shown for simplicity. For gels in Fig 3b, Fig 4a-c and Extended Data 4a-d, gels were cropped to show only lanes that are relevant to this study.
Replication	In all cases, experiments were conducted in biological duplicate or triplicate as is standard in the field. All attempts displayed similar agreements.
Randomization	This is not relevant to our study, as randomization is not used in small-scale studies in the field of molecular microbiology
Blinding	This is not relevant to our study, as blinding is not used in small-scale studies in the field of molecular microbiology

Reporting for specific materials, systems and methods

We require information from authors about some types of materials, experimental systems and methods used in many studies. Here, indicate whether each material, system or method listed is relevant to your study. If you are not sure if a list item applies to your research, read the appropriate section before selecting a response.

Materials & experimental systems

n/a	Involved in the study
☐	☒ Antibodies
☐	☒ Eukaryotic cell lines
☒	☐ Palaeontology
☒	☐ Animals and other organisms
☒	☐ Human research participants
☒	☐ Clinical data

Methods

n/a	Involved in the study
☒	☐ ChIP-seq
☒	☐ Flow cytometry
☒	☐ MRI-based neuroimaging

Antibodies

Antibodies used	Mouse anti-Myc (Cell Signaling Technology #2276), Rabbit anti-GST (Cell Signaling Technology #2625), Mouse anti-E.coli RNA Polymerase Beta (BioLegend #663903), HRP-conjugated Goat anti-Mouse IgG (Santa Cruz Biotechnology #sc-2005), HRP-conjugated Goat anti-Rabbit IgG (Bio-Rad #170-6515)
Validation	Primary antibodies (Mouse anti-Myc, Rabbit anti-GST and Mouse anti-E.coli RNA Polymerase Beta) were used at 1:5000 in TBS with 0.1% Tween20 and 5% nonfat dry milk for 1hr at room temperature or 16hrs at 4 degrees Celsius. Secondary antibodies (Goat anti-Mouse IgG and Goat anti-Rabbit IgG) were used similarly for 1hr at room temperature. Antibodies were validated by comparing western blot results to strains with no epitope.

Eukaryotic cell lines

Policy information about cell lines

Cell line source(s)	HEK 293T (ATCC)
Authentication	HEK 293T cells (ATCC) were authenticated by STR profiling
Mycoplasma contamination	All cell cultures tested negative for contamination; media supernatant from cell cultures were analyzed monthly for the mycoplasma using MycoAlert Plus (Lonza)
Commonly misidentified lines (See ICLAC register)	No commonly misidentified cell lines were used